european
surgery
ACA Acta Chirurgica Austriaca

Comparative analysis of custom-made endograft simulation techniques: physical prototypes versus numerical simulations

Fadi Taher ⬤ · Miriam Kliewer · Jean-Noel Albertini · Joris Vermunt · Raphael Doustaly · Corinna Walter · Markus Plimon · Jürgen Falkensammer · Herbert Langenberger · Afshin Assadian

Summary

Background The technical success of fenestrated endovascular aortic repair (FEVAR) relies on the exact fit of the custom-made endograft in the patient. Numerical simulation software has been made available (PLANOP™, PrediSurge) to digitally test the intended endograft design.

Methods The distance between opposite peaks of the proximal endograft sealing ring were measured on computed tomography (CT) scans of the test implantation within a 3D printed model, on numerical simulation software, and on postoperative CT (reference). Two types of modeling were used for the aorta in the numerical simulation software: rigid and deformable. This resulted in four measurements: (1) CT scan of the physical endograft prototype implanted in a rigid printed silicone model of the aorta, (2) rigid numerical or finite element (FE) simulation of the endograft implanted in a rigid aortic model, (3) numerical or FE simulation with a deformable virtual aortic model, and (4) patient postoperative CT.

Results Ten patients were included in the study. The mean distance between peaks was 26.8mm in the postoperative CT scan (reference). The distance in the rigid printed model was 23.8 ± 2.0 mm $p < 0.003$). The FE analysis with rigid aorta measured 23.8 ± 1.5 mm ($p < 0.006$). Measurements performed on CT of the physical prototype test implanted in the printed silicone model of the aorta, and measurements from FE analysis with rigid modeling, were not significantly different. Measurements in a simulated deformable aorta were 27.4 ± 2.1 mm ($p < 0.521$). A high correlation ($r = 0.81$, $p < 0.01$) was found between measurements on postoperative CT and deformable aorta FE analysis.

Conclusion Numerical simulation with a rigid aorta may be a suitable substitute for traditional test implantation of a non-sterile prototype within a 3D aortic model. This may help reduce time for graft planning and fabrication. The FE analysis with a deformable aorta was able to predict peak-to-peak distances at the proximal sealing ring more reliably. The effect on clinical outcomes and endoleak occurrence remains to be elucidated in future trials.

Keywords Fenestrated endovascular aortic repair · FEVAR · Numerical simulation · Finite element analysis · Custom-made device

Dr. F. Taher, M.D. (✉) · M. Kliewer, M.D. · C. Walter, M.D. · M. Plimon, M.D. · A. Assadian, M.D.
Department of Vascular and Endovascular Surgery, Hospital Ottakring Vienna, Montleartstr. 37, Pav. 30b, 1160 Vienna, Austria
fadi.taher@gmail.com

J.-N. Albertini, M.D.
Department of Vascular Surgery, CHU Saint-Etienne, Saint-Etienne, France

J. Vermunt, PhD · R. Doustaly, MSc
PrediSurge, Saint-Etienne, France

J. Falkensammer, M.D.
Department of Vascular Surgery, Barmherzige Brueder Hospital, Linz, Austria

H. Langenberger, M.D.
Department of Radiology, Hospital Ottakring Vienna, Vienna, Austria

Introduction

Custom-made endografts are an asset when treating aortic aneurysms that cannot be excluded using off-the-shelf devices. Fenestrated endovascular aortic repair (FEVAR) as a custom-made device is routinely used for the treatment of juxta- or pararenal aneurysms and to treat type Ia endoleaks [1, 2]. In
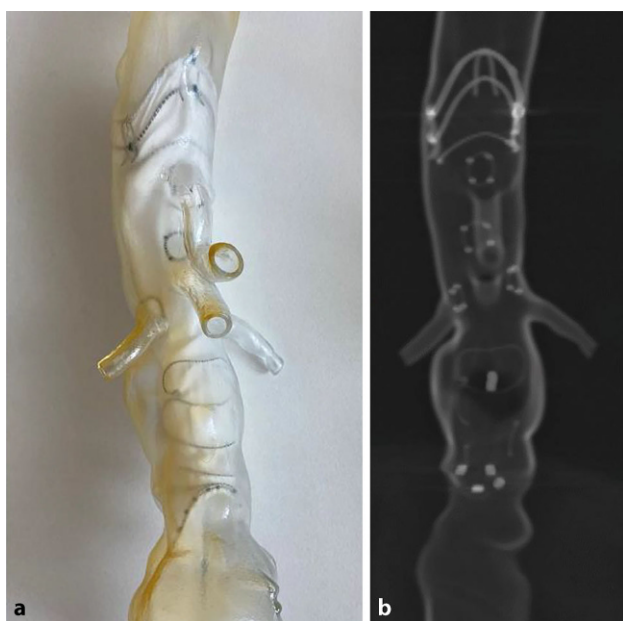
Fig. 1 Each pairing of a prototype and printed three-dimensional aortic model (**a**) was assessed for adequate alignment of the device and then mapped using a computed tomography angiography scan (**b**)

combination with a thoracic endograft, these devices have also been successfully used to treat thoracoabdominal aneurysms [3]. High success rates for various indications and applications have been reported in single- and multicenter trials [4–6].

Optimal technical results rely on a precise fit of the graft to the applicable aortic configuration. For the Terumo Aortic fenestrated Anaconda™ (Terumo Aortic, Inchinnan, Scotland, UK) device, a routine practice is to test-implant a non-sterile prototype of the device in a three-dimensional (3D) printed hard plastic model of a patient's aorta. Thus, a suitable fit in the patient can be ensured. A single-center study described the value of this test implantation during the device planning and fabrication phase [7].

This procedure, however, can be time-consuming and by no means can be regarded a guarantee for a perfect fit. More recently, a method has been described to use numerical simulation of the prototype and simulation of the patient aorta based on preoperative computed tomography angiography (CTA) imaging [8]. It was concluded that while being faster, numerical simulation using finite-element (FE) analysis was equivalent to the traditional way of test-implanting a prototype in a printed aortic model regarding precise positioning of fenestrations.

In the current study we applied the previously described FE analysis to a simulation of a deformable patient aorta and compared its ability to predict the proximal sealing ring configuration of the endograft in the patient. We therefore compared numerical simulation with postoperative CTA using the distance of proximal sealing ring peaks as a surrogate for the prox-

imal graft configuration. Measurements using simulation with rigid aorta modeling and CT of the corresponding rigid printed 3D prototypes as well as aortic models are also included in the analysis. The study thus aimed to identify the possible merit of assessing endograft fit within a deformable numerical simulation. The configuration of the proximal sealing ring as a relevant determinant of reliable exclusion of aortic pathology, and a possible factor to impact longevity of aortic repair, was therefore investigated as a surrogate of suitable fit of the custom-made device.

Materials and methods

Ethics statement

The present study was conducted in accordance with the Declaration of Helsinki and following review board approval of the investigation by the responsible ethics committee. Approval of the retrospective investigation included a waiver of informed consent.

Patients and pre- and postoperative computed tomography angiography imaging data

Imaging data from consecutive patients who underwent FEVAR at our Department of Vascular and Endovascular Surgery between 2019 and 2021 were accessed and reviewed. All endografts had been planned and produced based on 1-mm slice thickness CTA, and all patients had undergone postoperative CTA during their hospital stay. Preoperative CTA was used for FE analysis and a standard procedure had been used for 3D aortic model production before FEVAR surgery had been performed. All patients underwent routine postoperative CTA after FEVAR. Measurements from postoperative CTA were used as the reference. Measurements from prototype testing in the silicone model and measurements from the numerical simulations could thus be compared with the reference value from postoperative patient CTA.

Data from traditional test-implantation of non-sterile prototype in a printed 3D aortic silicone model

The 3D aortic silicone models used for endograft prototype testing with the included patients were retrieved and assessed visually. Prototype fit was adjusted in the model until all fenestrations matched up with vessel origins. A CT scan was then obtained for each individual prototype and aortic model pairing to allow for measurements using the same software as for postoperative CTA (Figs. 1 and 2).

Data from numerical simulations with rigid and deformable components

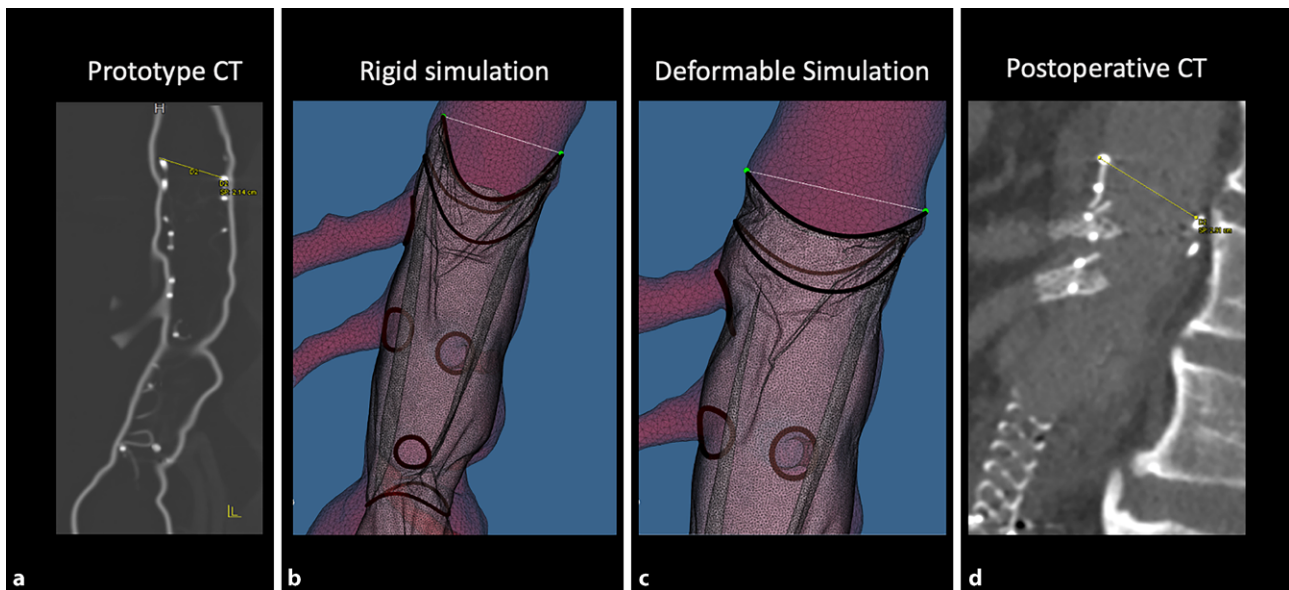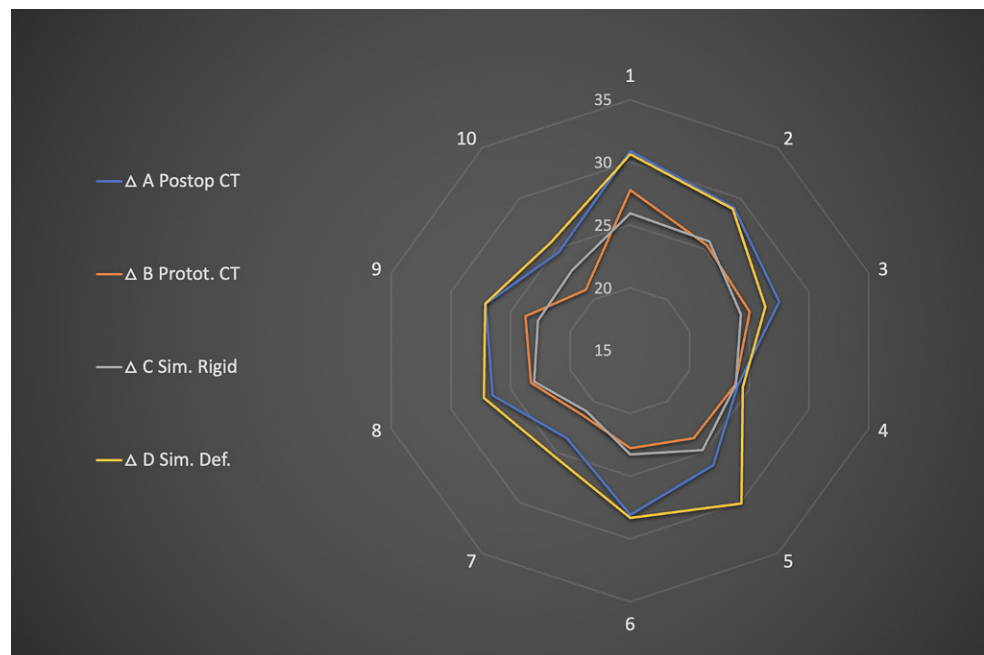The numerical simulations were performed using FE analyses (PLANOP™, PrediSurge, Saint-Etienne,

Fig. 2 Comparable measurements of the surrogate variable of distance between proximal sealing ring peaks as performed using a computed tomography scan of the prototype in the rigid silicone model (**a**), the rigid and deformable simulations (**b**, **c**), and the patient's postoperative computed tomography angiography (**d**)

Fig. 3 Spider chart illustrating, for each of the ten clinical cases included, agreement and differences between measurements. *Delta* and *scale* refer to the distance measured in millimeters and *outer numbering* designates the ten patients included. *CT* computed tomography, *Protot.* prototype and rigid printed aortic model pairing, *Sim.* simulation, *Def.* deformable

France) and according to the procedure outlined in a previous study in which simulations were performed for the same fenestrated device [8]. For the present study, numerical simulation was performed twice. First using a rigid aorta (which was expected to mimic the printed silicone model in a virtual fashion), and then also using a virtual simulation of a deformable aorta (which is hypothesized to better simulate how a real aorta would interact with the graft in patients). These distinctive properties of the two versions of simulations performed are further outlined in the next paragraph.

Simulation of a rigid aortic component was performed to act as a comparison for the 3D printed model, as well as to be compared with postoperative CTA measurements from patients. Simulation with a deformable aorta as an arguably more advanced technique was performed to better represent the graft–aorta interaction. Rigidity and elasticity as specified by both of the involved components, i.e., the graft and the aorta, were considered for this FE

Table 1 Summary of mean peak-to-peak measurements from sources

Peak-to-peak distance	Mean	SD	p	Comparison to postoperative computed tomography
A. Postoperative computed tomography angiography	26.8	2.3	Reference	Reference
B. Computed tomography of tested prototype in 3D aortic model	23.8	2.0	0.006	Significant
C. Rigid aorta numerical simulation	23.8	1.5	0.003	Significant
D. Deformable component aorta simulation	27.4	2.1	0.521	Not significant
SD standard deviation; *p* values are given for independent comparison of means using *t* test and postoperative computed tomography angiography as a reference				

analysis. The properties not only of the nitinol and fabric of the graft, but also of the vessel wall were divided into finite elements and their interactions were transformed into calculations by appropriate equations that consider the applicable properties of included materials and tissues.

Measurements from both numerical simulation techniques (rigid or deformable aorta) were compared with each other, with the rigid 3D printed silicone model-prototype pairing, as well as with measurements from postoperative patient CTA.

Measurement variable and technique

The distance between opposite peaks of the proximal sealing ring was defined as a reproducible and easy-to-measure target variable. It was intended to act as a surrogate of proximal sealing ring configuration. The measurement can be performed from multiple angles in the viewing agent of FE analysis simulations. On CT scans, measurement was performed leading-edge to leading-edge (LELE) on 3/2 sagittal and coronal plane reconstructions as well as on 1-mm axial cuts of the applicable CT studies. For demonstration purposes, 20-mm multiplanar reconstructions are included as representative images.

Statistical analysis

Means and standard deviations are reported for continuous measurements. An independent samples *t* test was performed to compare means between the different measurement sources of postoperative patient CTA (reference), CT scan of the prototype in a rigid 3D printed aortic model, and FE simulations with a rigid or deformable aorta. A spider graph is provided to visualize agreement and differences between the different sources for measurements. Linear regressions through the origin were performed to compute a proportionality coefficient between the tested measurements and the reference measurement. A Pearson correlation test was performed between measurements from the CT and FE analysis.

Results

Ten patients were included in the study. The mean distances between peaks were 26.8 ± 2.3 mm in the postoperative CT scan. The CT imaging of the prototype within the rigid printed model showed a mean distance of 23.8 ± 2.0 mm, with a mean absolute difference of 3.0 ± 1.2 mm compared to the reference. This difference was statistically significant ($p < 0.003$). The FE analysis with a rigid aorta resulted in a mean of 23.8 ± 1.5 mm, with a mean absolute difference of 0.8 ± 0.6 mm when compared with 3D printed model-derived measurements. Pearson's test showed a very high correlation between these two measurements ($r = 0.83$, $p < 0.003$). The mean distance between proximal sealing ring peaks in a simulation of endograft deployment with a deformable aorta was 27.4 ± 2.1 mm. The difference between distances from postoperative CT and the simulation with a deformable aortic model was not significant ($p = 0.521$), with a mean absolute difference of 1.0 ± 1.1 mm. Table 1 summarizes the mean measurements and *p* values from comparisons between CT and FE analysis. Figure 3 illustrates the agreement and differences between measurements for each of the included FEVAR case within a spider chart. A very high correlation between measurements extracted from numerical simulation with deformable aorta and measurements from postoperative CT was observed (correlation coefficient $r = 0.81$, $p = 0.004$). Scatterplots in Fig. 4 display the correlation between measurements derived from numerical simulation with a deformable aorta and prototype test in 3D-printed model versus the postoperative CT reference. Linear regression through the origin shows a coefficient of 1.02 between measurements from numerical simulation and postoperative CT.

Discussion

The present study provides additional evidence of the possible usefulness of numerical simulation over the traditional use of a demo device and 3D aortic model in custom-made endograft planning. The merit of a fit test of a custom-made graft prototype seems logical and has previously been shown in a study investigating the effect of prototype-testing in a 3D aortic model before FEVAR [7]. With advanced technologies at our disposal and an option to simulate such a test through numerical simulation, we can verifiably reduce delivery times of custom-made endografts [8]. In that regard, numerical simulation already has the potential of a positive impact on patients undergoing FEVAR treatment by being able to reduce the waiting time for surgery. The current study investigated not only whether numerical simulation can reproduce a measurement on the traditional fit test in a rigid aortic

Fig. 4 Numerical simulation of a deformable aorta shows good correlation with measurements from postoperative computed tomography angiography
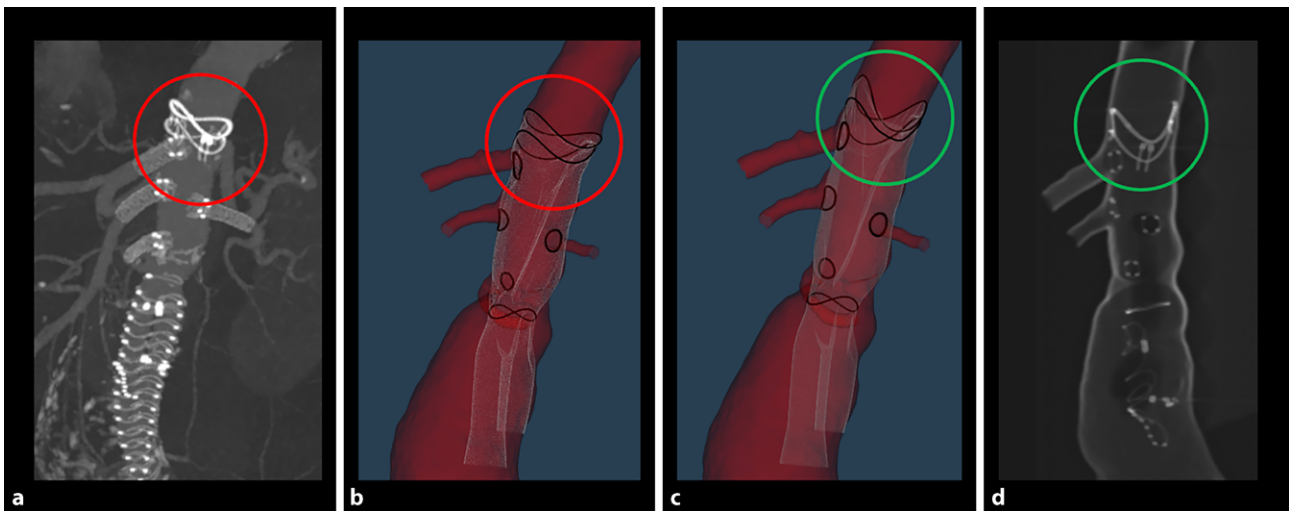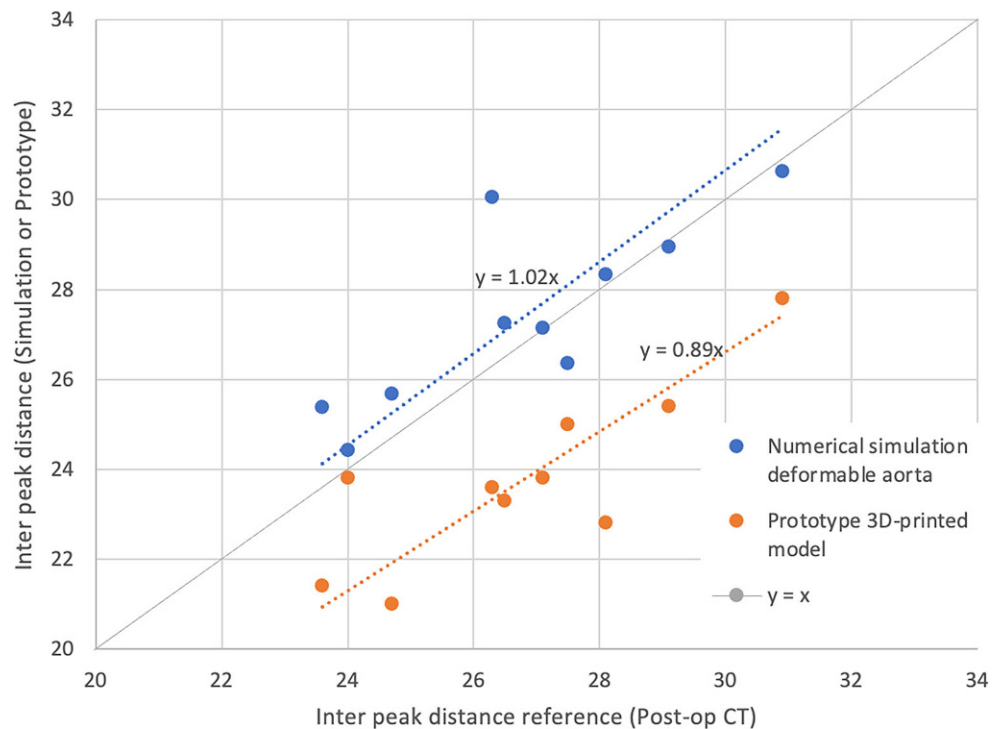

Fig. 5 Postoperative computed tomography angiography (**a**) shows less tension within the proximal sealing rings. This can also be seen on deformable simulation (**b**) as indicated by the red circles. In comparison, rigid simulation (**c**) and the printed silicone model (**d**) show a different proximal sealing ring configuration (green circles)

model, but also whether using a deformable simulation of the aorta may have an added benefit.

While agreement between the rigid printed and simulated models regarding peak-to-peak measurements at the proximal sealing ring was apparent, both modalities were significantly different from measurements in postoperative CTA. However, a good correlation between measurements from FE analysis with a deformable aorta and postoperative CT was demonstrated and the observed mean absolute difference between the two was close to 1 mm. It is therefore likely that testing the graft in a deformable simulated model of the aorta may allow for more accurate assessments of graft–aorta interactions, which have previously been reported to occur after FEVAR [9].

This work constitutes to the authors' best knowledge the first FE analysis in which the interaction of a custom-made fenestrated device with a deformable modeling of the patient's aorta is assessed. Future investigations may build on the encouraging results of this study to include additional demographic and clinical patient data and assess the relevance in terms of clinical outcome. Apart from a previously de-

scribed advantage of saving time, simulation—when performed using the deformable aortic and graft components—may be able to assess the adequacy and reliability of sizing [10, 11] and oversizing, and potentially be able to identify favorable configurations of the proximal sealing ring (Fig. 5). Stent graft sizing using numerical simulation has previously also been reported to be a success in patients undergoing FEVAR using a differently designed custom-made graft [12]. The simulation procedure is by no means limited to the pararenal setting or specific endografts used in this series [13, 14]. As the proximal sealing ring typical to the Anaconda endograft is likely a factor relevant for the longevity of the endovascular repair achieved using this specific device, correlation of the findings from FE analysis with deformable components with mid- to long-term clinical results and occurrence of endoleaks or loss of sealing ring tension may also be worthwhile topics for future trials.

Limitations

The study was conducted with a small sample of patients and may be considered hypothesis-generating rather than a definitive proof of the value of numerical simulation for assessing custom-made endograft design. The parameter chosen to assess graft–aorta interaction (peak-to-peak distance) was selected due to its simplicity and reproducibility, as well as the potential to provide a substitute that can easily be assessed on the models, simulations, and CT scans. It is merely one metric that may be considered when assessing the fit of a custom-made endograft, and its use in this study is based on the notion that the proximal sealing ring is an important area when it comes to graft–aorta interactions and the desired seal when performing FEVAR using this device.

Conclusion

When a deformable model of the aorta is computed, numerical simulation seems reliable and superior to printed rigid aortic models in predicting proximal sealing ring configurations as a surrogate of endograft fit and endograft–aorta interaction in the patient. This deserves further assessment in future trials that investigate a possible benefit of fewer proximal sealing zone failures. Finite element analysis may be able to streamline communication during endograft planning and fabrication, save time, and improve our ability to ensure adequate fit of custom-made devices in our patients.

References

1. Karelis A, Haulon S, Sonesson B, Adam D, Kolbel T, Oderich G, et al. Editor's choice—multicentre outcomes of redo fenestrated/branched endovascular aneurysm repair to rescue failed fenestrated endografts. Eur J Vasc Endovasc Surg. 2021;62(5):738–45.
2. Oderich GS, Greenberg RK, Farber M, Lyden S, Sanchez L, Fairman R, et al. Results of the United States multicenter prospective study evaluating the Zenith fenestrated endovascular graft for treatment of juxtarenal abdominal aortic aneurysms. J Vasc Surg. 2014;60(6):1420–8.e1–5.
3. Falkensammer J, Taher F, Plimon M, Kliewer M, Walter C, Pelanek E, et al. Assessment of pull-out forces in TEVAR and ANACONDA FEVAR combination and early clinical results: creation of a proximal landing zone for FEVAR in patients with extent I and extent IV TAAas. Ann Vasc Surg. 2020;66:160–70.
4. de Niet A, Zeebregts CJ, Reijnen M, Fenestrated Anaconda Study group. Outcomes after treatment of complex aortic abdominal aneurysms with the fenestrated Anaconda endograft. J Vasc Surg. 2020;72(1):25–35.e1.
5. Oderich GS, Farber MA, Schneider D, Makaroun M, Sanchez LA, Schanzer A, et al. Final 5-year results of the United States Zenith fenestrated prospective multicenter study for juxtarenal abdominal aortic aneurysms. J Vasc Surg. 2021;73(4):1128–38.e2.
6. Taher F, Assadian A, Strassegger J, Duschek N, Koulas S, Senekowitsch C, et al. Pararenal aortic ulcer repair. Eur J Vasc Endovasc Surg. 2016;51(4):504–10.
7. Taher F, Falkensammer J, McCarte J, Strassegger J, Uhlmann M, Schuch P, et al. The influence of prototype testing in three-dimensional aortic models on fenestrated endograft design. J Vasc Surg. 2017;65(6):1591–7.
8. Kliewer ME, Bordet M, Chavent B, Reijnen M, Frisch N, Midy D, et al. Assessment of fenestrated anaconda stent graft design by numerical simulation: results of a European prospective multicenter study. J Vasc Surg. 2022;75(1):99–108.e2.
9. de Niet A, Donselaar EJ, Holewijn S, Tielliu IFJ, Lardenoije J, Zeebregts CJ, et al. Endograft conformability in fenestrated endovascular aneurysm repair for complex abdominal aortic aneurysms. J Endovasc Ther. 2020;27(5):848–56.
10. Banno H, Kobeiter H, Brossier J, Marzelle J, Presles E, Becquemin JP. Inter-observer variability in sizing fenestrated and/or branched aortic stent-grafts. Eur J Vasc Endovasc Surg. 2014;47(1):45–52.
11. Malkawi AH, Resch TA, Bown MJ, Manning BJ, Poloniecki JD, Nordon IM, et al. Sizing fenestrated aortic stent-grafts. Eur J Vasc Endovasc Surg. 2011;41(3):311–6.
12. Derycke L, Senemaud J, Perrin D, Avril S, Desgranges P, Albertini JN, et al. Patient specific computer modelling for automated sizing of fenestrated stent grafts. Eur J Vasc Endovasc Surg. 2020;59(2):237–46.
13. Demanget N, Duprey A, Badel P, Orgeas L, Avril S, Geindreau C, et al. Finite element analysis of the mechanical performances of 8 marketed aortic stent-grafts. J Endovasc Ther. 2013;20(4):523–35.
14. Derycke L, Perrin D, Cochennec F, Albertini JN, Avril S. Predictive numerical simulations of double branch stent-graft deployment in an aortic arch aneurysm. Ann Biomed Eng. 2019;47(4):1051–62.